Journal of Electronic Imaging

JElectronicImaging.org

Demosaicking with adaptive reference range selection

Bo-Gyu Park
Hyun-Gyu Lee
Sang-Chul Lee

Bo-Gyu Park, Hyun-Gyu Lee, Sang-Chul Lee, "Demosaicking with adaptive reference range selection," *J. Electron. Imaging* **28**(1), 013021 (2019), doi: 10.1117/1.JEI.28.1.013021.

Journal of Electronic Imaging 28(1), 013021 (Jan∕Feb 2019)

Demosaicking with adaptive reference range selection

Bo-Gyu Park, Hyun-Gyu Lee, and Sang-Chul Lee*
INHA University, Department of Computer Engineering, Incheon, Republic of Korea

Abstract. Image demosaicking is a method of reconstructing an RGB image from a Bayer pattern, which is required when color information is lacking because a single charge-coupled device is used during the image extraction process of a digital camera. There are many restrictions on the reconstruction of a Bayer image to an RGB image. Given that each pixel contains only one-color information, artifacts, such as false color or the zipper effect, may occur at the edges, which can arise as a result of significant differences in brightness and color change. We propose a demosaicking method for adaptively selecting the reference range of color difference to obtain reliable information from texture regions and reconstructing into the RGB image. In particular, we determine the adaptive weight and reference range for four directions, east (E), west (W), south (S), and north (N), to improve the reliability of the color pixel obtained by a color difference estimation using guided filtering applied on residuals. In our experiment, we compare the results of the proposed method for the Kodak and IMAX datasets with those of nine demosaicking methods. The proposed method shows similar or improved results in terms of the color peak signal-to-noise ratio. In addition, compared to other methods, the visual quality improved by reducing residual artifacts. © *2019 SPIE and IS&T* [DOI: 10.1117/1.JEI.28.1.013021]

Keywords: residual; guided filtering; color difference; reference-range; false color; zipper effect.

Paper 180463 received May 24, 2018; accepted for publication Jan. 3, 2019; published online Feb. 4, 2019.

1 Introduction

Demosaicking is a process of reconstructing the Bayer image acquired from a charge-coupled device (CCD) into a complete RGB image defined by three color channels, red (R), green (G), and blue (B). Bayer images typically suffer from artifacts, such as false color or the zipper effect, because of insufficient color information resulting from the structural limitations of the CCD. Zipper effects and false color occur on edges that have significant differences in pixel value changes. Many researchers have approached the artifact removal problem using various methods.[1–3] A demosaicking method was proposed for reducing artifacts in which pixel information is reconstructed in the estimated edge direction based on the gradient.[4,5] Gradient-based methods are effectively applied to most edge directions, but artifacts increase due to poor reliability of gradient computations in textured regions with frequent changes in brightness and chrominance.[6,7]

Several approaches have also been suggested for converting the brightness and chrominance space into the frequency domain.[8–14] In frequency domain-based studies, antialiasing filters were designed to remove noise in the frequency domain of a Bayer image or a reconstructed RGB image. The noise removal results were then used to analyze the relationship between the frequencies of each channel and between high and low frequencies. Frequency analysis has two advantages: efficiency in edge classification and impressive performance of the filter designed for the intercorrelation of each channel. However, in the case of images with weak correlations between colors, the performance of filters designed for cross correlation is reduced, and the artifact rate is increased.

In addition, several methods analyze human color perception, such as the CIELab color model, color differences, such as R–G and B–G, and the color ratio for the linear change characteristics between channels.[4,15–19] These methods apply spectral correlation for similar structures such as texture or edges. A method based on homogeneity in the CIELab color space determined the interpolation in the horizontal or vertical direction by associating the pixels at the current position with the surrounding pixels.[20] The methods of using color difference, color ratio, and color perception have been utilized in many studies as they are capable of recovering images easily and efficiently.

Recently, a method of extracting color difference information based on residual difference using guided filtering[21] was proposed. It showed faster computation, a higher color peak signal-to-noise ratio (CPSNR), and an improved artifact removal rate compared to recent methods.[22–26] Color difference information extraction based on residuals can reflect the characteristics of texture or edges using the values of other channels at locations without specific color information.

However, using conventional methods, it is difficult to reflect the texture information of various objects in the image using only a fixed reference area. In this paper, we propose a demosaicking method based on the adaptive reference range determination of color difference using the extraction of residual color difference information.[22] As shown in Fig. 1, the proposed method determines the weights and reference ranges of color difference in four directions, namely, east (E), west (W), south (S), and north (N), for contents at the respective pixels. Reconstruction based on estimated color difference compensates for the limitations of the previous techniques for extracting residual-based color difference information. The proposed method makes the following two contributions:

*Address all correspondence to Sang-Chul Lee, E-mail: sclee@inha.ac.kr

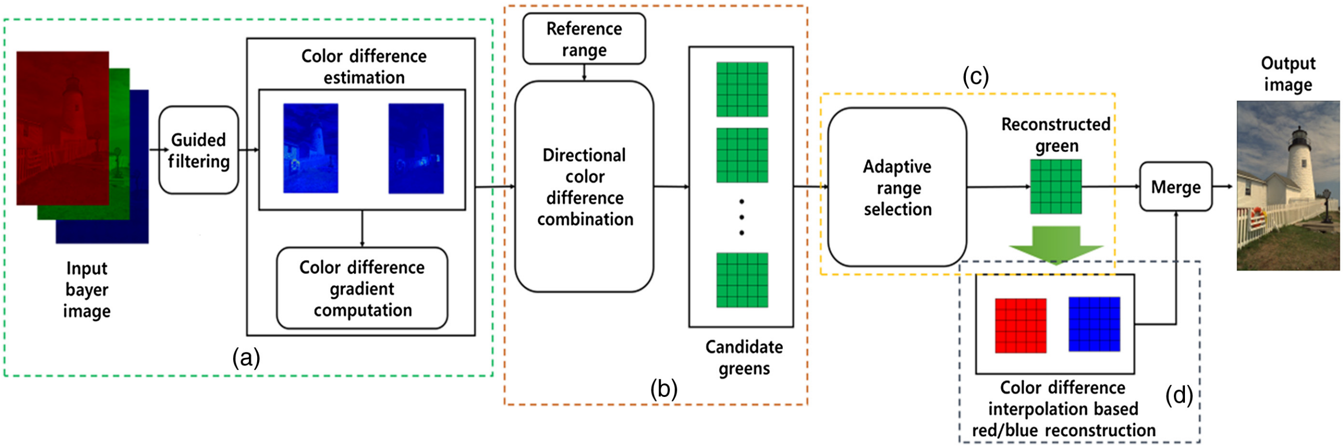

Fig. 1 Overall flow diagram of the proposed method. (a) Residual-based color difference extraction and gradient calculation for input Bayer images, (b) calculation of the optimum G channel estimation value according to the reference range for the east, west, south, and north directions, (c) estimation of the final G channel value using the optimum reference range selection criterion, and (d) color difference-based R and B restoration with estimated G channel.

- Unlike previous methods, the reference pixel area is not fixed in this paper, and therefore, the estimated value is closer to the ground truth.
- The artifact removal rate is improved by adaptively selecting a reference area of color difference suitable for local content in the object.

2 Background

2.1 *Extraction of Residual-Based Color Difference Information*

This section briefly introduces the technique for residual-based color difference extraction, residual interpolation (RI), proposed in Ref. 22, which was used as a color difference extraction technique in this study. First, we reconstruct the G-band using bilinear interpolation. Then, the R-band used by the interpolated G-band is reconstructed as follows:

$$\tilde{G}^{\mathrm{H}}_{i,j} = (G_{i,j-1} + G_{i,j+1})/2, \quad \tilde{G}^{\mathrm{V}}_{i,j} = (G_{i-1,j} + G_{i+1,j})/2$$
$$\tilde{R}^{\mathrm{H}} = T_{\mathrm{GF}}(b_{\mathrm{R}}, \tilde{G}^{\mathrm{H}}), \tag{1}$$

where i and j are the positions of the target pixel, $\tilde{G}^{\mathrm{H}}$ and $\tilde{G}^{\mathrm{V}}$ are the G values reconstructed using bilinear interpolation in the horizontal and vertical directions, $\tilde{R}^{\mathrm{H}}$ is the estimated R value for the horizontal direction using $\tilde{G}^{\mathrm{H}}$ as a guide image, b_{R} is the R value in the Bayer image, and T_{GF} is the guided filtering for the target image by the guide image.

We first compute the residuals between the Bayer R value and the interpolated R-band and then compute the color difference. The residual is used to reconstruct a clearer R-band using Eq. (2). The color difference is computed between the interpolated G-band and the interpolated R-band. The residuals and the color difference are defined as follows:

$$\hat{R}^{\mathrm{H}}_{i,j} = \frac{[b_R(i,j-1) - \tilde{R}^{\mathrm{H}}_{i,j-1}]}{2} + \frac{[b_R(i,j+1) - \tilde{R}^{\mathrm{H}}_{i,j+1}]}{2} + \tilde{R}^{\mathrm{H}}_{i,j}, \tag{2}$$

$$d^{\mathrm{H}}_{\mathrm{G,R}} = \hat{G}^{\mathrm{H}}_{\mathrm{R}} - R \quad \text{or} \quad G - \hat{R}^{\mathrm{H}}_{\mathrm{G}}, \quad d^{\mathrm{H}}_{\mathrm{G,B}} = \hat{G}^{\mathrm{H}}_{\mathrm{B}} - B \quad \text{or} \quad G - \hat{B}^{\mathrm{H}}_{\mathrm{G}}$$
$$d^{\mathrm{V}}_{\mathrm{G,R}} = \hat{G}^{\mathrm{V}}_{\mathrm{R}} - R \quad \text{or} \quad G - \hat{R}^{\mathrm{V}}_{\mathrm{G}}, \quad d^{\mathrm{V}}_{\mathrm{G,B}} = \hat{G}^{\mathrm{V}}_{\mathrm{B}} - B \quad \text{or} \quad G - \hat{B}^{\mathrm{V}}_{\mathrm{G}}, \tag{3}$$

where $\hat{G}^{\mathrm{H}}_{\mathrm{R}}$ is the G value at the R pixel position, $\hat{R}^{\mathrm{H}}_{\mathrm{G}}$ is the R value at the G pixel, and d^{H} and d^{V} are the color difference information for the horizontal and vertical directions, respectively.

Figure 2 shows the reconstruction of the R-channel values using color difference based on bilinear interpolation and guided filtering. A bilinear interpolation-based method is a simple and effective means of estimating the color difference and involves calculating the color difference for the bilinear interpolated G and the original R or B values. However, in the case of regions with significant changes in pixel values, it is difficult to detect a change in the pixel unit in the interpolated image using bilinear interpolation. Therefore, the error at the G value propagates more when the R and B channels are reconstructed using the reconstructed G channel. Conversely, the method for estimating the residual-based color difference[22] interpolates the R value using the bilinear interpolated G value as a guide image through guided filtering. The difference between the interpolated R channel and the original R value is represented by the residual. This residual, in turn, is combined with the interpolated R channel by guided filtering to estimate a more reliable R channel value. The residual-based reconstruction method solves the problem of the propagation of the errors in the color difference estimation based on the bilinear interpolation, thus allowing more reliable color difference information to be extracted.

The process of estimating the residual-based color difference is shown in Fig. 2. First, bilinear interpolation is performed on the G channel in the horizontal and vertical directions. Then, the R channel is reconstructed using the reconstructed G channel as a guide image, as shown in Eq. (1). As shown in Eq. (2), the difference between the R value in the reconstructed R channel image in the horizontal and vertical directions and the original R

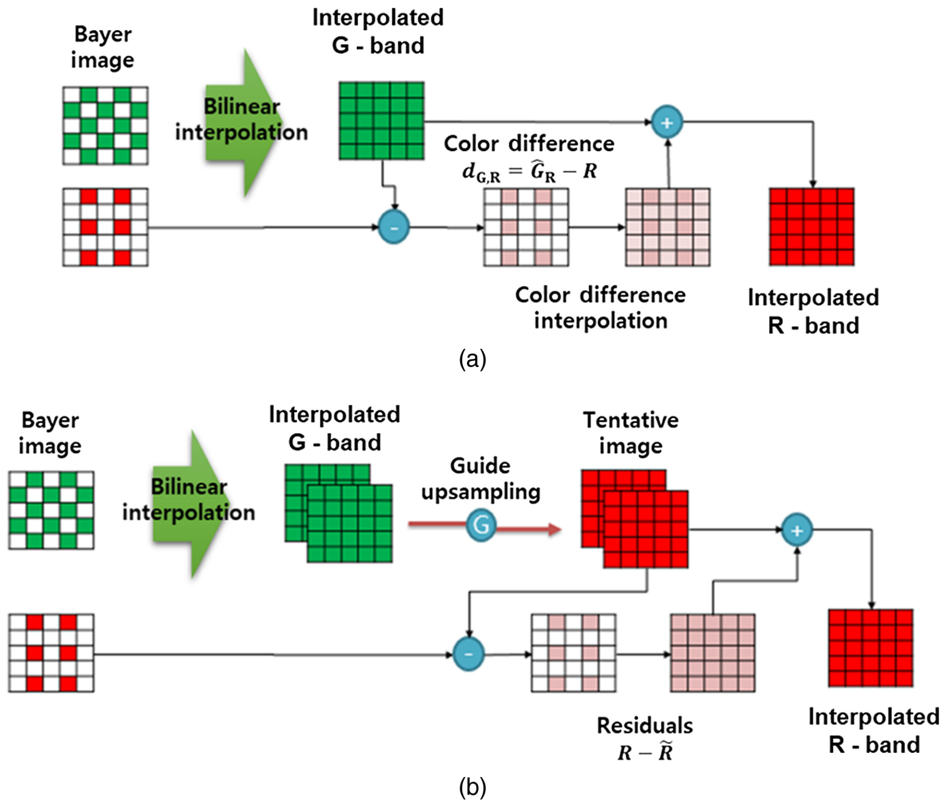

Fig. 2 (a) Demosaicking by bilinear interpolation-based color difference estimation by Eq. (3), and (b) residual-based demosaicking by guided filtering.

value in the Bayer image is defined as the residual. The residual is added to the reconstructed $\tilde{R}$ in the horizontal and vertical directions to obtain an image with a reduced error rate. The color difference information between the G channel and the R and B channels for horizontal and vertical orientations is evaluated by the finally estimated R, G, and B values.

3 Adaptive Reference Range-Based Interpolation

3.1 *Adaptive Reference Range Selection*

The estimation of the color difference values for the horizontal and vertical directions of the corresponding pixel positions calculated using Eq. (3) include a large error because of the incorrect reflection of the information in the excessively complicated texture region. To solve this problem, the RI method uses the gradient-based threshold-free (GBTF) algorithm[6] to reduce the color difference error in the four directions, E, W, S, and N. GBTF is the algorithm to decide the adaptive threshold for target pixel using the gradient of color difference. The threshold is set for the combination of four directional gradients of color difference for all neighbor pixels in a 5×5 mask. Since this algorithm considers four-directional neighbor pixels in the target position, it produces better results in edge or texture regions. However, GBTF makes it difficult to guarantee reliability when numerous contents are mixed within a fixed reference range. In this paper, we propose extending the fixed reference range in GBTF to an adaptively selected reference range to estimate reliable color difference information in various content areas.

Algorithm 1 describes the final G value determination through adaptive reference range selection. At each pixel position, the reference range is gradually increased for selecting the reference range suitable for the contents, and the reconstruction candidate value is estimated. The estimation of the final color difference value at each pixel position considers the four directions, E, W, N, and S; the weight for each direction is defined by the average of the gradients. The value $\hat{G}_r$ is estimated by the final color difference considering directionality in each reference range. It is used as a candidate for the final G value selection.

As shown in Fig. 3, the color difference reference range r is sequentially increased in the four directions, E, W, S, and N, at each pixel position for the horizontal and vertical color difference values d^{H} and d^{V}. In addition, the average color difference values $\overline{d}_r^{H,E}$, $\overline{d}_r^{H,W}$, $\overline{d}_r^{V,S}$, and $\overline{d}_r^{V,N}$ and the average values of the color difference gradients $\overline{\Delta d}_r^{H,E}$, $\overline{\Delta d}_r^{H,W}$, $\overline{\Delta d}_r^{V,S}$, and $\overline{\Delta d}_r^{V,N}$ are calculated for each direction. The final color difference $\hat{d}_r^{H}$ and $\hat{d}_r^{V}$ for the horizontal and vertical directions, respectively, in each reference range r is estimated using Eq. (4). Then, the final candidate G value in our proposed method (ARS) is calculated. The results of the previous studies[6,16,24] show a similar performance, excluding the artifacts at the edges. We performed the reconstruction by selecting G_r close to the results of the comparison methods. In the area of possible artifacts, at least one of the values reconstructed through the reference range has a value similar to that of the G value in the original image, and this value is close to the values in the artifact area of the existing studies. Thus, the reference range r with the smallest difference from

Algorithm 1 Adaptive reference range selection.

---

procedure ADAPTIVE_RANGE_SELECTION (b_c, d_r, G^{target})

Variable description:

b_c: pixel at color c on Bayer pattern

r: reference range (pixel)

o: reference direction {N, S, E, W}

Δd: Gaussian filtered gradient of color differences

Candidate green channels estimation:

for $r \leftarrow 0$, 8 **do**

$\overline{d}_r^o = \frac{1}{r+1}\sum_{i=0}^{r} d_i^o$ for each direction o

$\overline{\Delta d}_r^o = \frac{1}{r+1}\sum_{i=0}^{r} \Delta d_i^o$ for each direction o

$w_r^{\text{H,E}} = \frac{\overline{\Delta d}_r^{\text{H,W}}}{\overline{\Delta d}_r^{\text{H,E}}+\overline{\Delta d}_r^{\text{H,W}}}$

$w_r^{\text{H,W}} = \frac{\overline{\Delta d}_r^{\text{H,E}}}{\overline{\Delta d}_r^{\text{H,E}}+\overline{\Delta d}_r^{\text{H,W}}}$

if $\overline{\Delta d}_r^{\text{H,E}} > \overline{\Delta d}_r^{\text{H,W}}$ and $\frac{\overline{d}_r^{\text{H,W}}}{\overline{d}_r^{\text{H,E}}} < 0$, then $\hat{d}_r^{\text{H}} = -\overline{d}_r^{\text{H,W}} w_r^{\text{H,E}} + \overline{d}_r^{\text{H,W}} w_r^{\text{H,W}}$

else if $\overline{\Delta d}_r^{\text{H,E}} \le \overline{\Delta d}_r^{\text{H,W}}$ and $\frac{\overline{d}_r^{\text{H,W}}}{\overline{d}_r^{\text{H,E}}} < 0$, then

$\hat{d}_r^{\text{H}} = \overline{d}_r^{\text{H,W}} w_r^{\text{H,E}} - \overline{d}_r^{\text{H,W}} w_r^{\text{H,W}}$

else if $\left\{\overline{\Delta d}_r^{\text{H,E}} > \overline{\Delta d}_r^{\text{H,W}} \text{ and } \frac{\overline{d}_r^{\text{H,W}}}{\overline{d}_r^{\text{H,E}}} \ge 0\right\}$ or $\left\{\overline{\Delta d}_r^{\text{H,E}} \le \overline{\Delta d}_r^{\text{H,W}} \text{ and } \frac{\overline{d}_r^{\text{H,W}}}{\overline{d}_r^{\text{H,E}}} \ge 0\right\}$,

then $\hat{d}_r^{\text{H}} = \overline{d}_r^{\text{H,W}} w_r^{\text{H,E}} + \overline{d}_r^{\text{H,W}} w_r^{\text{H,W}}$

$\overline{\Delta d}_r^{\text{H}} = \min(\overline{\Delta d}_r^{\text{H,E}}, \overline{\Delta d}_r^{\text{H,W}})$, $\overline{\Delta d}_r^{\text{V}} = \min(\overline{\Delta d}_r^{\text{V,N}}, \overline{\Delta d}_r^{\text{V,S}})$

$w_r^{\text{H}} = \frac{\overline{\Delta d}_r^{\text{V}}}{\overline{\Delta d}_r^{\text{H}}+\overline{\Delta d}_r^{\text{V}}}$

$w_r^{\text{V}} = \frac{\overline{\Delta d}_r^{\text{H}}}{\overline{\Delta d}_r^{\text{H}}+\overline{\Delta d}_r^{\text{V}}}$

$\hat{G}_r^{\text{R}} = b_{\text{R}} + w_r^{\text{V}}\hat{d}_r^{\text{H}} + w_r^{\text{H}}\hat{d}_r^{\text{V}}$

$\hat{G}_r^{\text{B}} = b_{\text{B}} + w_r^{\text{V}}\hat{d}_r^{\text{H}} + w_r^{\text{H}}\hat{d}_r^{\text{V}}$

end for

Minimized distance selection:

$\hat{G} = \min_{\hat{G}_r}(G_{i,j}^{\text{target}} - \hat{G}_r)$

return $\hat{G}$

end procedure

---

the G channel value G_r at the current pixel position is estimated by weight calculation for each of the horizontal and vertical color differences using Eq. (5). The reconstructed result in the target method is selected. Finally, we use $\hat{G}$ selected by r as the final G channel value:

$$w_r^{\text{H,E}} = \frac{\overline{\Delta d}_r^{\text{H,W}}}{\overline{\Delta d}_r^{\text{H,E}}+\overline{\Delta d}_r^{\text{H,W}}},\ w_r^{\text{H,W}} = \frac{\overline{\Delta d}_r^{\text{H,E}}}{\overline{\Delta d}_r^{\text{H,E}}+\overline{\Delta d}_r^{\text{H,W}}}$$

$$\hat{d}_r^{\text{H}} = \begin{cases} -\overline{d}_r^{\text{H,W}} w_r^{\text{H,E}} + \overline{d}_r^{\text{H,W}} w_r^{\text{H,W}}, & \text{if } \overline{\Delta d}_r^{\text{H,E}} > \overline{\Delta d}_r^{\text{H,W}} \text{ and } \frac{\overline{d}_r^{\text{H,W}}}{\overline{d}_r^{\text{H,E}}} < 0 \\ \overline{d}_r^{\text{H,W}} w_r^{\text{H,E}} + \overline{d}_r^{\text{H,W}} w_r^{\text{H,W}}, & \text{if } \overline{\Delta d}_r^{\text{H,E}} > \overline{\Delta d}_r^{\text{H,W}} \text{ and } \frac{\overline{d}_r^{\text{H,W}}}{\overline{d}_r^{\text{H,E}}} \ge 0 \\ \overline{d}_r^{\text{H,W}} w_r^{\text{H,E}} - \overline{d}_r^{\text{H,W}} w_r^{\text{H,W}}, & \text{if } \overline{\Delta d}_r^{\text{H,E}} \le \overline{\Delta d}_r^{\text{H,W}} \text{ and } \frac{\overline{d}_r^{\text{H,W}}}{\overline{d}_r^{\text{H,E}}} < 0 \\ \overline{d}_r^{\text{H,W}} w_r^{\text{H,E}} + \overline{d}_r^{\text{H,W}} w_r^{\text{H,W}}, & \text{if } \overline{\Delta d}_r^{\text{H,E}} \le \overline{\Delta d}_r^{\text{H,W}} \text{ and } \frac{\overline{d}_r^{\text{H,W}}}{\overline{d}_r^{\text{H,E}}} \ge 0 \end{cases} \tag{4}$$

where r is the number of pixels as the reference range, $w_r^{\text{H,E}}$ and $w_r^{\text{H,W}}$ are the weight values for the referenced color differences in both horizontal directions, and $\hat{d}_r^{\text{H}}$ is the color difference value for the horizontal direction calculated by satisfying the condition in Eq. (4). The calculation of the color difference value $\hat{d}_r^{\text{V}}$ for the vertical direction is the same as that of $\hat{d}_r^{\text{H}}$. The optimal G value $\hat{G}$ at the current pixel position is determined by considering the relationship between the current pixel and the surrounding area, and G_r is selected for the optimal reference range r for the current position. In this case, the optimal reference range r is obtained by comparing the current pixel position with the target pixel value, reconstructed as in the foundation methods, and the r with the smallest difference between the target pixel and G_r is selected. The comparison methods[6,11,16,22–24,27] are used to compare with candidate G value in our proposed method (ARS). The results of the previous studies[6,16,24] show a similar performance, excluding the artifacts at the edges. We perform the reconstruction by selecting G_r close to the results of the comparison methods. In the area of possible artifacts, at least one of the values reconstructed through the reference range has a value similar to that of the G value in the original image, and this value is close to the values in the artifact area of the previous studies. Using this fact, the reference range r with the smallest difference from the G channel value G_r at the current pixel position is estimated by weight calculation for each of the horizontal and vertical color differences using Eq. (5). Then, the reconstructed result in the target method is selected. Finally, we use $\hat{G}$ selected by r as the final G channel value:

$$\overline{\Delta d}_r^{\text{H}} = \min(\overline{\Delta d}_r^{\text{H,E}}, \overline{\Delta d}_r^{\text{H,W}}), \quad \overline{\Delta d}_r^{\text{V}} = \min(\overline{\Delta d}_r^{\text{V,N}}, \overline{\Delta d}_r^{\text{V,S}})$$
$$w_r^{\text{H}} = \frac{\overline{\Delta d}_r^{\text{V}}}{\overline{\Delta d}_r^{\text{H}}+\overline{\Delta d}_r^{\text{V}}}, \quad w_r^{V} = \frac{\overline{\Delta d}_r^{\text{H}}}{\overline{\Delta d}_r^{\text{H}}+\overline{\Delta d}_r^{\text{V}}}$$
$$\hat{G}_r^{\text{R}} = R + w_r^{\text{V}}\hat{d}_r^{\text{H}} + w_r^{\text{H}}\hat{d}_r^{\text{V}}, \quad \hat{G}_r^{\text{B}} = B + w_r^{\text{V}}\hat{d}_r^{\text{H}} + w_r^{\text{H}}\hat{d}_r^{\text{V}}, \tag{5}$$

$$\hat{G} = \min_{\hat{G}_r}(G_{i,j}^{\text{target}} - \hat{G}_r), \tag{6}$$

where $\overline{\Delta d}_r^{\text{H}}$ and $\overline{\Delta d}_r^{\text{V}}$ are the average color difference gradient values with minimum change in the horizontal and vertical directions, respectively, and w_r^{H} and w_r^{V} are the weight values. $\hat{G}_r$ is the estimated G value in each reference range, G^{target} is the result of applying comparison methods on the

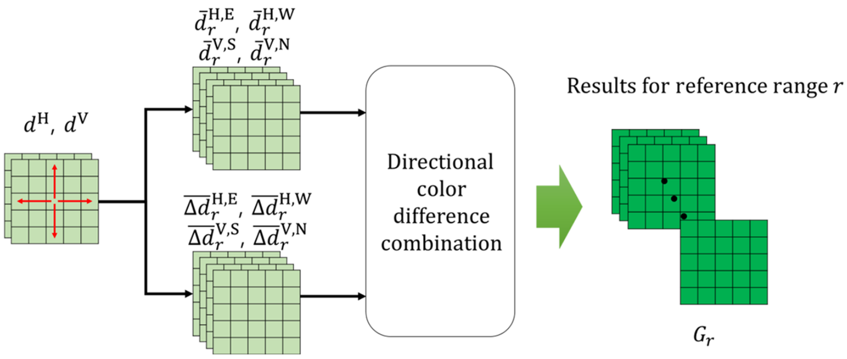

Fig. 3 Candidate G channel estimation flow suitable for texture change where the adaptive reference range is applied to the color difference information estimated as in Ref. 21; the color difference at the current pixel position is estimated by considering the average color difference and the average color difference gradient for the east, west, south, and north directions.

selection criteria, and $\hat{G}$ is determined to be the final G channel value. $\hat{G}$ is used as a reference for color difference estimation and interpolation direction determination in the reconstruction of the R and B channels.

3.2 *R and B Channel Reconstruction Techniques*

3.2.1 *R value reconstruction at B pixel location*

Reconstruction of the R value at B channel pixels is alternately performed as bilinear interpolation. The R pixels at the B pixel position exist diagonally in the directions north east (NE), north west (NW), south east (SE), and south west (SW), and the R value to be reconstructed is the average of the values at the four positions. The color difference value at the center position is estimated using the color difference between the value of the G channel reconstructed in the previous step and R having the original color value in the Bayer image and is defined by $d_{\mathrm{R,G}} = \mathrm{R} - \hat{G}$. The value of R is reconstructed by summing the G value with the color difference at the center. The B value at the R pixel position is reconstructed in the same manner.

3.2.2 *R and B value reconstruction at G pixel location*

Figure 4(a) shows that the reconstruction at the R or B pixel position is classified as a horizontal or vertical distribution pattern depending on the position of R or B having the original color. First, the color differences $d_{\mathrm{R,G}}$ and $d_{\mathrm{B,G}}$ are calculated at the position shaded orange. To estimate the linear interpolation order of the computed color difference, horizontal and vertical gradients ΔG_x and ΔG_y for the reconstructed G are calculated. The interpolation order is decided for the determined direction by calculating the average gradients $\Delta\overline{G}_x$ and $\Delta\overline{G}_y$ of the 5×5 patch size for the calculated gradient. As shown in Fig. 4(b), when the value of $\Delta\overline{G}_x$ is smaller than $\Delta\overline{G}_y$, we interpolate it first in the horizontal direction and then in the vertical direction to determine the color difference at the central position.

Figure 4(b) shows the case where $\Delta\overline{G}_x$ of the vertical pattern is smaller than $\Delta\overline{G}_y$. Here, the final color difference value is determined by interpolation in the horizontal direction. Conversely, if $\Delta\overline{G}_y$ is smaller, the interpolation order is determined as shown in Fig. 4(b). The color difference of the blank position is interpolated in the vertical direction and thereafter interpolated again horizontally. The final color difference is estimated by the upper and lower portions of the central position. The same mechanism is applied in the case of a horizontal pattern. In addition, to compensate for the disadvantages of the proposed gradient-based R and B pixel reconstruction, the reconstruction error of the edge is reduced using the reconstructed R and B pixel by applying a Laplacian-based method with minimized-Laplacian residual interpolation (MLRI):[23]

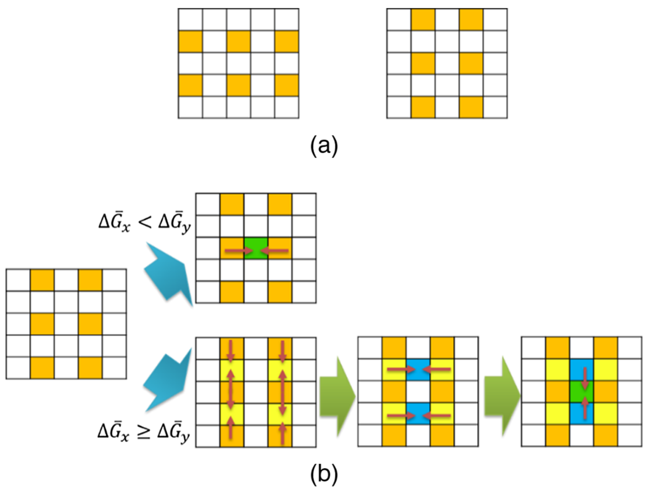

Fig. 4 (a) Distribution pattern of R or B at the G pixel position and (b) example of interpolation steps by mean gradient for a vertical distribution pattern.

$$\hat{R} = (\mathrm{R_{ARS}} + \mathrm{R_{MLRI}})/2 \quad \hat{B} = (\mathrm{B_{ARS}} + \mathrm{B_{MLRI}})/2, \tag{7}$$

where $\mathrm{R_{ARS}}$ is the result of the R pixel reconstruction of the proposed method, and $\mathrm{R_{MLRI}}$ is the result of the R reconstruction of the MLRI method. The final reconstructed value $\hat{R}$ is defined as the average of $\mathrm{R_{ARS}}$ and $\mathrm{R_{MLRI}}$. The same process is applied to obtain the final reconstructed $\hat{B}$ value.

4 Experimental Results

Our experiments were performed using two representative datasets, Kodak PhotoCD and IMAX high-quality images. A total of nine conventional research methods, adaptive homogeneity-directed (AHD), alternating projections (AP), directional linear minimum mean-square error estimation (DLMMSE), residue interpolation (RI), minimized-Laplacian residue interpolation (MLRI), adaptive residue interpolation (ARI), directional difference regression (DDR), fused regression (FR), and gradient-based threshold-free (GBTF), and the proposed method were tested and compared in terms of their qualitative evaluation, based on the comparison and analysis of image quality, and quantitative evaluation, according to the CPSNR.[28] CPSNR is the average mean square error (MSE) of the reconstructed color components for RGB values normalized to [0, 1].

Recently, some research studies have often used pansharpening, shorthand for panchromatic sharpening.[29] It is a process of merging high-resolution panchromatic and lower resolution multispectral imagery to create a single high-resolution color image. The panchromatic image is produced to a high-resolution image by three or four, or more, low-resolution multispectral bands. As shown in Fig. 5, the ARS is applied to three cases. Its input can be either the RGB image produced by other demosaicking methods, the average of the Malvar-He-Cutler (MHC), or the average of other demosaicked RGB images.

In this paper, the panchromatic image is constructed by the average of the demosaicked images. It has the information needed for the reconstructed image from the R, G, and B color bands. Pansharpening produces a panchromatic image, but its computational cost is higher than the G-band approach due to the demosaick image. The G-band approach has less information to demosaick an image because of the low correlation between the G-band and R/B-band. So, we performed the comparative experiments for the G-band and the panchromatic image.

Recent research[30–32] has obtained a reconstructed image using CFA 2.0 that is composed of red, green, blue, and white. However, their experimental environment is not a fair evaluation because they used CFA 2.0 type, not the standard CFA type that we tested. Hence, they were not tested. In all the experiments, padding was applied to achieve a fair performance analysis considering the different reference window sizes of the research methods.

4.1 *Experimental Setup*

To increase the reliability of the reflection of the texture information per area, the reference range was divided into nine steps from 0 to 8. We effectively reconstructed values for various texture areas. As shown in Fig. 6, we tested by

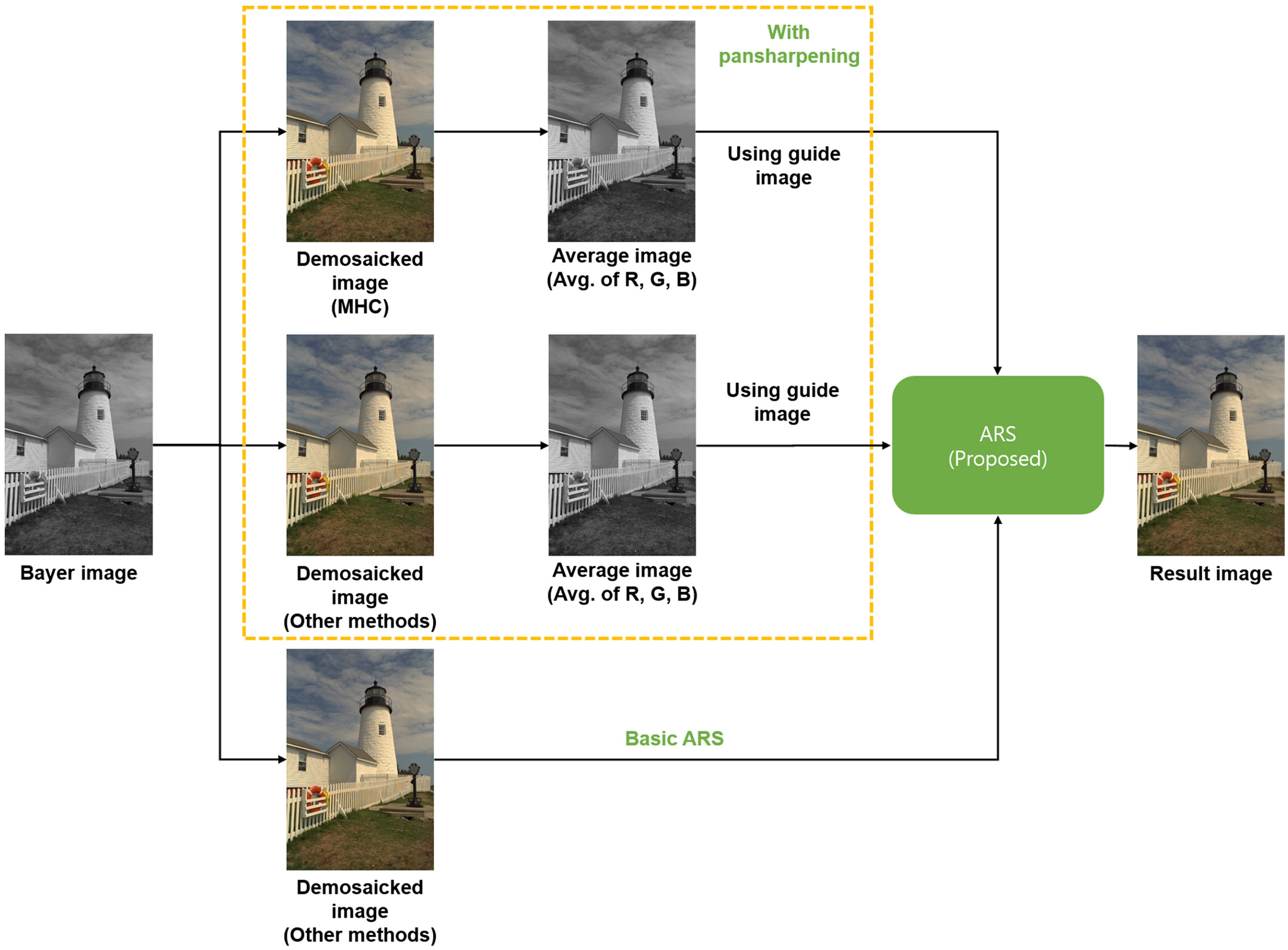

Fig. 5 The illustration of relationship between ARS and pansharpening. The input of ARS is RGB image produced by demosaicking methods or the average of the demosaicked RGB image.

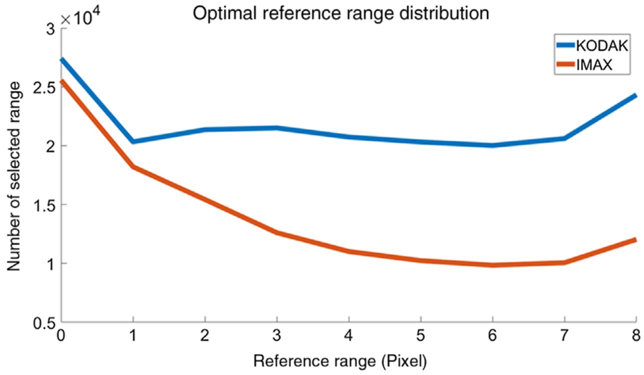

Fig. 6 Distribution graph of reference-ranges with values most similar to those of the original image in the Kodak dataset (24 images) and IMAX dataset (18 images). The horizontal axis represents the color difference reference range for the east, west, south, and north directions from 0 to 8 and the vertical axis represents the average number of selections for the reference range of each dataset.

selecting the optimal reference range for a Kodak dataset (24 images) and IMAX dataset (18 images). The small reference range between 0 and 3 is suitable for images with a high color saturation, such as those in the IMAX dataset, where frequent rapid color changes are largely detected even within the same object. However, for the Kodak dataset, having overall low saturation and insignificant changes in the same object, a uniform range of reference between 0 and 8 is suitable.

4.2 *Quantitative Evaluation*

We compared the quantitative evaluation by demosaicking the results for 42 images from both the Kodak and IMAX datasets. Tables 1 and 2 show a comparison of the average CPSNR of the proposed methods and comparison methods. In the table, bold characters indicate the highest value in each column. The comparison methods in italics use the same type of color difference calculation method.[22,23] The demosaicking method, using the determination of the optimal reference range of the proposed method, demonstrated overall better results than those obtained using previous methods. In the case of the Kodak dataset, the average CPSNR for AHD increased up to 1.57 dB, and the average CPSNR for all other methods increased up to 0.58 dB. In the case of the IMAX dataset, an increase of 1.19 dB compared to AP and an overall increase of 0.72 dB compared to the results of nine methods were observed. Figure 7 shows a comparison of the average CPSNR for all datasets; the proposed method achieved improved results compared to the comparison methods. Because the ARS applies the color difference for the reference range, the higher the contrast, the larger the error propagation. The overall scores of the Kodak dataset were higher due to having lower contrast images.

In Tables 1 and 2, columns 3 and 4 show the results applied to the color difference by the panchromatic image used as the guide image. Column 3 shows the panchromatic image made by the average of the demosaicked images of the MHC method. While column 4 shows the panchromatic image made by the average of the demosaicked images of the comparison methods. Since most comparison methods reconstructed better quality images than MHC, the panchromatic images made by the comparison methods possess information closer to the original than the MHC. ARS generates estimated G values for the reference ranges (0 to 8). They can represent various values with propagation errors in context. Most estimated values are closer to the original value than some methods such as AHD. However, they have fewer good values than some methods including ARI and FR as most values estimated by the latter two are fairly close to the original. Hence, the values produced by the ARS were lower than the original values produced by ARI or FR.

Table 3 shows a comparison of the average execution time. The execution time with ARS was longer than 12

Table 1 Average CPSNR results for the Kodak datasets. Among the comparison methods, those in italics present the method estimated by the same color difference. The CPSNR results show the best value in each column. Text in italic signifies values that are lower than those of the comparison methods and text in bold shows an improved quantitative value.

Methods	Comparison methods (without ARS)	With ARS	With ARS + Pansharpening (MHC)	With ARS + Pansharpening (avg. of R,G,B using comparison methods)
AHD[4]	37.78	39.35 (**1.57**)	39.31 (**1.53**)	38.31 (**0.53**)
AP[11]	39.07	39.96 (**0.89**)	39.26 (**0.19**)	39.33 (**0.26**)
DLMMSE[26]	40.14	40.77 (**0.63**)	39.96 (*0.18*)	41.03 (**0.89**)
RI[33]	38.55	39.25 (**0.70**)	39.26 (**0.71**)	39.70 (**1.15**)
MLRI[22]	39.58	39.74 (**0.16**)	39.40 (*0.18*)	40.00 (**0.42**)
ARI[23]	39.74	40.33 (**0.59**)	39.79 (**0.05**)	40.31 (**0.57**)
GBTF[6]	40.62	40.38 (*0.24*)	39.64 (*0.98*)	40.54 (*0.08*)
DDR[16]	40.26	40.81 (**0.56**)	40.02 (*0.24*)	40.93 (**0.67**)
FR[16]	***41.08***	***41.45*** (**0.37**)	***40.37*** (*0.71*)	***41.69*** (**0.61**)

Table 2 Average CPSNR results for the IMAX dataset.

Methods	Comparison methods (without ARS)	With ARS	With ARS + Pansharpening (MHC)	With ARS + Pansharpening (avg. of R,G,B using comparison methods)
AHD[4]	33.52	35.59 (**2.07**)	35.09 (**1.57**)	35.21 (**1.69**)
AP[11]	33.06	34.25 (**1.19**)	33.86 (**0.80**)	33.29 (**0.23**)
DLMMSE[26]	34.50	37.06 (**2.56**)	35.82 (**1.32**)	36.56 (**2.06**)
RI[33]	36.51	36.61 (**0.10**)	35.66 (*0.85*)	36.57 (**0.06**)
MLRI[22]	36.65	36.42 (*0.23*)	35.64 (*1.01*)	36.38 (*0.27*)
ARI[23]	***37.54***	37.06 (*0.48*)	35.85 (*1.69*)	37.14 (*0.04*)
GBTF[6]	34.41	34.91 (**0.50**)	34.62 (**0.21**)	34.59 (**0.18**)
DDR[16]	35.53	36.47 (**0.94**)	35.55 (**0.02**)	35.80 (**0.27**)
FR[16]	37.50	***37.34*** (*0.16*)	***35.95*** (1.55)	***37.85*** (**0.35**)

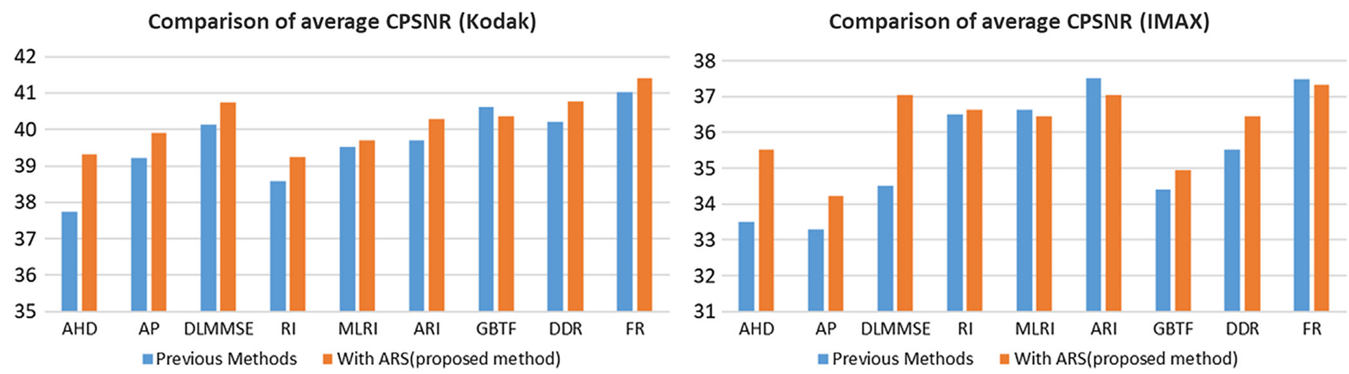

Fig. 7 Average CPSNR results for the Kodak and IMAX datasets. The CPSNR is improved compared to that of related studies.

Table 3 Execution time results for the Kodak and IMAX datasets.

Method	Comparison methods (without ARS)		With ARS (proposed)	
	Kodak	IMAX	Kodak	IMAX
AHD[4]	1.79	1.92	14.18	9.07
AP[11]	0.96	0.55	13.41	8.39
DLMMSE[26]	3.41	2.19	15.82	10.06
RI[33]	1.24	0.77	13.64	8.64
MLRI[22]	1.96	1.24	14.35	9.12
ARI[23]	49.57	30.49	61.95	38.34
GBTF[6]	4.77	3.10	17.18	10.91
DDR[16]	7.66	4.79	20.05	12.67
FR[16]	23.22	14.79	35.62	22.65

and 8 s compared with the comparison methods for the Kodak and IMAX datasets, respectively. However, this time can be reduced by replacing the red and blue reconstruction parts in other ways.

4.3 *Qualitative Evaluation*

The artifact removal performance was also analyzed for some results of each method. In Fig. 8, the top left image is the original image and the first row shows the results of the comparison methods; the second row shows the proposed method; the third row shows the results of the pansharpening approach with MHC; the fourth row shows the pansharpening approach with comparison methods. It can be seen that the artifacts generated by the comparison methods either disappeared or were minimized when the proposed method with the pansharpening approach of the comparison methods was applied. Although the methods using the same color difference information estimation processes, such as RI, MLRI, ARI, DDR, and FR, showed a low artifact generation rate, our approach demonstrated improved results.

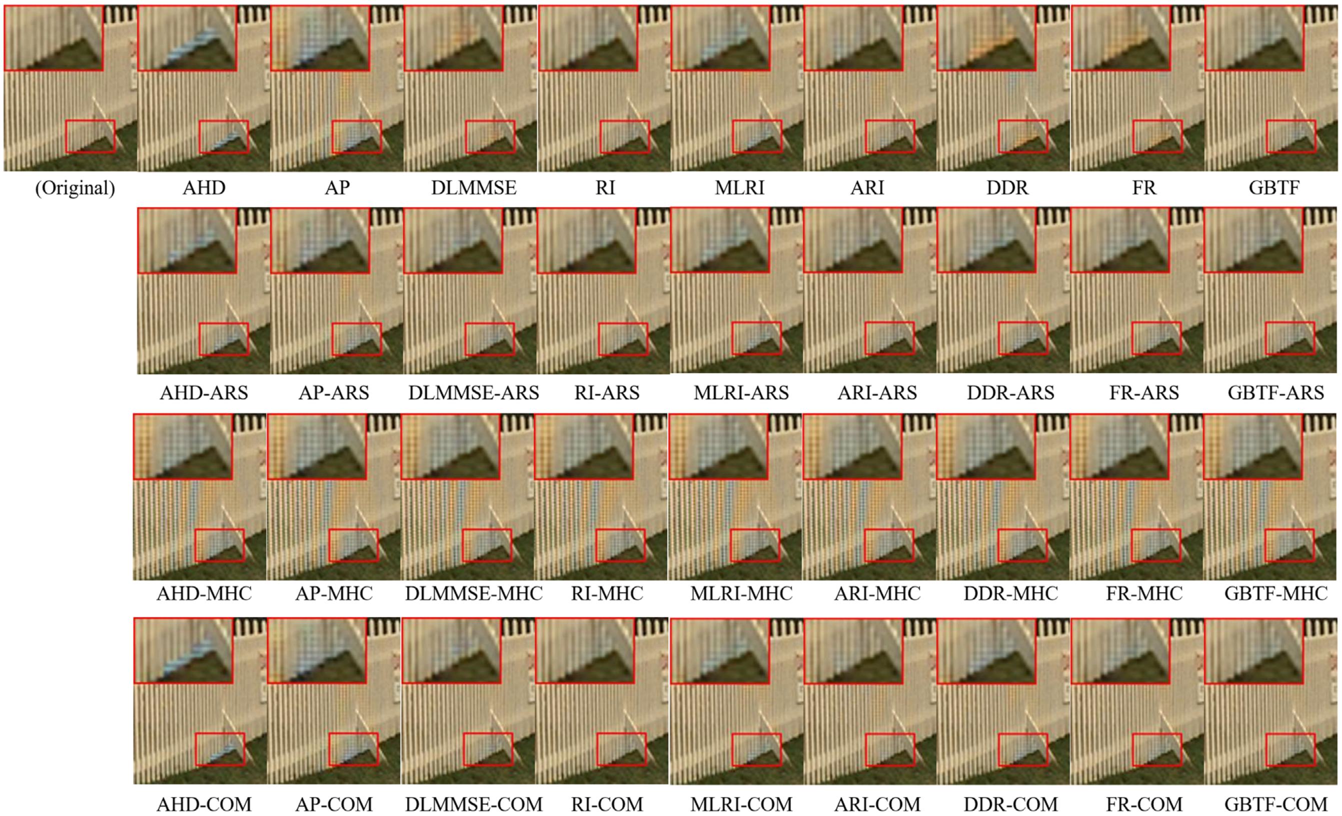

Fig. 8 Results of comparison methods and the proposed methods; the images in the first row are the results of the comparison methods (AHD, AP, DLMMSE, RI, MLRI, ARI, DDR, FR, and GBTF), the images in the second row are ARS results, the images in the third row are the results of the proposed methods with the panchromatic image of MHC, and the images in the fourth row are the results of the proposed method with the panchromatic image of the comparison methods. The results in (b) show that many artifacts occur in the fence but can be considerably eliminated by the proposed method. The improvement in the image quality of the proposed method is shown by the removal of the artifacts from the results of the most recent methods, as seen in MLRI, ARI, and DDR. The results of the third row show that many artifacts occur in the fence, but can be eliminated by ARS with a pan image of the comparison methods.

5 Conclusion

We proposed an adaptive reference range selection method using a guided filtering-based color difference estimation technique. The proposed method effectively removes the artifacts generated in the demosaicking process. In related studies, attempts were made to reconstruct an RGB image using a fixed reference range with color difference information. In the proposed method, more reliable reconstruction results were obtained by determining the weight of the color difference information for each direction and selecting the reference range of the color difference information adaptively. Moreover, ARS uses RGB or gray images as input images, so it can be applied to all demosaicking methods. Compared to the nine comparison methods, for datasets such as Kodak and IMAX, the average CPSNR and artifact reduction resulted in improved image quality. The proposed method is more robust to regional changes than comparison approaches, because it adapts the determination of the reference range for color difference information.

Acknowledgments

This work was supported by Inha University Research Grant.

References

1. B. K. Gunturk et al., "Demosaicking: color filter array interpolation," *Signal Process.* **22**, 44–54 (2005).
2. X. Li, B. Gunturk, and L. Zhang, "Image demosaicing: a systematic survey," *Proc. SPIE* **6822**, 68221J (2008).
3. M. Guarnera, G. Messina, and V. Tomaselli, "Adaptive color demosaicing and false color removal," *J. Electron. Imaging* **19**(2), 021105 (2010).
4. L. Zhang et al., "Color demosaicking by local directional interpolation and nonlocal adaptive thresholding," *J. Electron. Imaging* **20**(2), 023016 (2011).
5. A. Jasmine and J. Peter, "Multiscale gradients based directional demosaicing," in *IJERA Int. Conf. Humming Bird*, Vol. 3, pp. 30–36 (2014).
6. I. Pekkucuksen and Y. Altunbasak, "Gradient based threshold free color filter array interpolation," in *Int. Conf. Image Process. (ICIP)*, pp. 137–140 (2010).
7. J. F. Hamilton, Jr. and J. E. Adams Jr., "Adaptive color plan interpolation in single sensor color electronic camera," U.S. Patent 5,629,734 (1976).
8. D. Paliy et al., "Spatially adaptive color filter array interpolation for noiseless and noisy data," *Int. J. Imaging Syst. Technol.* **17**(3), 105–122 (2007).
9. K. Hirakawa, X. L. Meng, and P. J. Wolfe, "A framework for wavelet-based analysis and processing of color filter array images with applications to denoising and demosaicing," in *Int. Conf. Acoust. Speech and Signal Process.*, Vol. 1, pp. 597–600 (2007).
10. L. Fang et al., "Joint demosaicing and subpixel-based down-sampling for Bayer images: a fast frequency-domain analysis approach," *IEEE Trans. Multimedia* **14**(4), 1359–1369 (2012).

11. B. K. Gunturk, Y. Altunbasak, and R. M. Mersereau, "Color plane interpolation using alternating projections," *IEEE Trans. Image Process.* **11**(9), 997–1013 (2002).
12. Z. Sadeghipoor, Y. M. Lu, and S. Susstrunk, "Correlation-based joint acquisition and demosaicing of visible and near-infrared images," in *Int. Conf. Image Process. (ICIP)* (2011).
13. S. C. Pei and Y. Z. Hsiao, "Demosaicking of color filter array patterns using Quaternion Fourier transform and low pass filter," in *Int. Symp. Circuits and Systems (ISCAS)* (2013).
14. J. Liang et al., "Wavelet frame based color image demosaicing," *Inverse Prob. Imaging* **7**(3), 777–794 (2013).
15. K. H. Chung and Y. H. Chan, "Color demosaicing using variance of color differences," *IEEE Trans. Image Process.* **15**(10), 2944–2955 (2006).
16. J. Wu, R. Timofte, and V. Gool, "Demosaicing based on directional difference regression and efficient regression priors," *IEEE Trans. Image Process.* **25**(8), 3862–3874 (2016).
17. H. S. Malvar, L. He, and R. Cutler, "High quality linear interpolation for demosaicing of Bayer-patterned color images," in *Int. Conf. Acoust., Speech, and Signal Process. (ICASPP)*, Vol. 34, No. 11, pp. 2274–2282 (2004).
18. X. Li, "Demosaicing by successive approximation," *IEEE Trans. Image Process.* **14**(3), 370–379 (2005).
19. R. Ramanath et al., "Demosaicking methods for Bayer color arrays," *J. Electron. Imaging* **11**(3), 306–315 (2002).
20. K. Hirakawa and T. W. Parks, "Adaptive homogeneity directed demosaicking algorithm," *IEEE Trans. Image Process.* **14**(3), 360–369 (2005).
21. K. He, J. Sun, and X. Tang, "Guided image filtering," *Lect. Notes Comput. Sci.* **6311**, 1–14 (2010).
22. D. Kiku et al., "Residual interpolation for color image demosaicking," in *Int. Conf. Image Process. (ICIP)*, pp. 2304–2308 (2013).
23. D. Kiku et al., "Minimized-Laplacian residual interpolation for color image demosaicking," *Proc. SPIE* **9023**, 90230L (2014).
24. Y. Monno et al., "Adaptive residual interpolation for color image demosaicking," in *IEEE Conf. Image Process.*, pp. 3861–3865 (2015).
25. C. Kwan et al., "Demosaicing enhancement using pixel level fusion," *Signal Image Video Process.* **12**(4), 749–756 (2018).
26. M. Gharbi et al., "Deep joint demosaicking and denoising," *ACM Trans. Graphics* **35**(6), 191 (2016).
27. L. Zhang and X. Wu, "Color demosaicking via directional linear minimum mean square-error estimation," *IEEE Trans. Image Process.* **14**(12), 2167–2178 (2005).
28. R. Lukac, *Single-Sensor Imaging: Methods and Applications for Digital Cameras*, pp. 385–386, CRC Press, Florida (2008).
29. C. Zhang et al., "Universal demosaicking of color filter arrays," *IEEE Trans. Image Process.* **25**(11), 5173–5186 (2016).
30. C. Kwan et al., "Debayering RGBW color filter arrays: a pansharpening approach," in *Ubiquitous Comput., Electron. and Mobile Commun. Conf. (UEMCON)*, pp. 94–100 (2017).
31. K. Wachira, E. Mwangi, and G. Jeon, "An ordinal direction driven gradient-based RGBW CFA demosaicking technique using a bayerisation process and polyomino theory," in *IEEE AFRICON*, pp. 209–214 (2017).
32. M. Rafinazari and E. Dubois, "Demosaicking algorithms for RGBW color filter arrays," *Electron. Imaging* **2016**, 1–6 (2016).
33. W. Ye and K. K. Ma, "Color image demosaicing using iterative residual interpolation," *IEEE Trans. Image Process.* **24**(12), 5879–5891 (2015).

Biographies of the authors are not available.